Vision Research 76 (2013) 105–113

Contents lists available at SciVerse ScienceDirect

Vision Research

journal homepage: www.elsevier.com/locate/visres

Chronic delivery of low-level exogenous current preserves retinal function in pigmented P23H rat

Safa Rahmani, Les Bogdanowicz *, Joel Thomas, John R. Hetling

Department of Bioengineering, University of Illinois at Chicago, United States

ARTICLE INFO

Article history:
Received 3 July 2012
Received in revised form 26 October 2012
Available online 9 November 2012

Keywords:
Retinal degeneration
P23H rat
Transcorneal electrical stimulation
TES
Sensitivity
Phototransduction

ABSTRACT

Diffuse electrical currents delivered to the eye were investigated in a rat model of retinitis pigmentosa for potentially therapeutic effects. Low-level currents were passed between electrodes placed on the cornea and in the mouth during 30-min sessions two times per week from 4 to 16 weeks of age. Single-flash electroretinograms (ERG) were recorded and analyzed for amplitude and measures of sensitivity, and basic histology was performed. ERG a-wave amplitudes were slightly greater in treated vs. age-matched controls at 16 weeks of age, but the combined thicknesses of the outer nuclear layer and outer segment layer were similar at this age. Treated animals exhibited a significant preservation of b-wave amplitudes, and a striking preservation of rod sensitivity, measured as the stimulus strength required to reach half-saturation of the a-wave. Analysis of the leading edge of the a-wave using a delayed Gaussian function revealed a decrease in the parameter reflecting gain of the phototransduction cascade over the 12-week course of treatment, and no significant change in control animals over the same period. These results suggest that while the exogenous currents failed to preserve the number or gross structure of rods, the responsivity of individual photoreceptors was relatively preserved, perhaps via an increase in efficiency of photon capture (R^*/photon). This preserved functionality may delay the retraction of bipolar cell dendrites from degenerating photoreceptors.

1. Introduction

Retinitis pigmentosa (RP) and age-related macular degeneration (AMD) are two classes of eye diseases characterized by progressive cell loss and network remodeling in the retina, resulting in partial or total blindness (Marc et al., 2003). Principal therapies under investigation include pharmacology, gene therapy, and transplantation. Here we investigate the use of exogenous electrical currents delivered to the eye for potentially therapeutic effects. A transgenic animal model that exhibits a mutation and retinal degeneration similar to autosomal dominant retinitis pigmentosa (adRP,) the pigmented line 1 P23H rat, was used.

1.1. Precedent for electrical stimulation therapy

The effects of applied "sub-threshold" electric fields and currents on cells and tissues are relatively understudied. Fundamental studies have investigated directed growth of several cell types *in vitro* (e.g. PC12 cells; Cork et al., 1994). Subsequently, others investigated the ability of applied electric fields to direct regenerating spinal neurons, especially into artificial guidance structures (Borgens, 1999; Cheng & Lin, 2004). The application of exogenous electric fields has been shown to have significant effects on healing and regeneration in several different tissues, including periodontal bone (Kubota et al., 1995), skin (Ojingwa & Isseroff, 2002), peripheral motor nerves (Brushart et al., 2002), muscle afferents (Marqueste et al., 2004), spinal neurons (Borgens, Blight, & McGinnis, 1987; Borgens & Bohnert, 1997), and spiral ganglion cells (Leake et al., 1991). Al-Majed, Tam, and Gordon (2004) demonstrated that electrical stimulation accelerated and enhanced the expression of many regeneration-associated genes in rat femoral motor neurons. Leake, Hradek, and Snyder (1999) demonstrated that chronic electrical stimulation by a cochlear implant promoted survival of spiral ganglion neurons after neonatal deafness (in cats).

Positive effects of exogenous currents have been elicited under a wide range of experimental conditions. The *in vivo* studies listed above involved excitable as well as non-excitable tissues. In cases of excitable tissue, the effective applied electric fields were both above threshold for activating the target tissue or below threshold. The wave shape of the applied voltage (or current) varied from near DC (pulses of >1 s) to biphasic square pulses on the order of tens of microseconds in duration. The predominant guiding factors for selection of stimulus parameters have been empirical evidence bounded by safe limits (avoidance of heat, electrochemical, or electroporation injury due to application of an electric field). Recently, the parameter space of electrical stimulation (pulse duration,

* Corresponding author. Address: Department of Bioengineering, University of Illinois at Chicago, 851 South Morgan Street, Chicago, IL 60607-7052, United States.
E-mail address: Les.bogdanowicz@gmail.com (L. Bogdanowicz).

0042-6989/$ - see front matter © 2012 Elsevier Ltd. All rights reserved.
http://dx.doi.org/10.1016/j.visres.2012.10.016

stimulation frequency, duration of stimulation sessions, pulse kinetics) was explored systematically to find optimal values to promote survival of axotomized retinal ganglion cells (Morimoto et al., 2010).

Cho and colleagues have done extensive work to characterize the effect of exogenous electric fields on cell motility and modulation of intracellular calcium concentration *in vitro* (Cho et al., 2000, 2002; Khatib, Golan, & Cho, 2004; Sun & Cho, 2004; Sun, Wise, & Cho, 2004). For a variety of cell types (fibroblasts, macrophages, osteoblasts), the measured response to stimulation showed a strong dependence on frequency of the sinusoidal electric field. The greatest effects were elicited at frequencies between 1 and 10 Hz; increasing the frequency only as high as 20 Hz resulted in a near complete elimination of the measured effects. In cultured retinal Muller cells exposed to 20 Hz biphasic square pulses, increased IGF-1 transcription, intracellular calcium concentration, and BDNF expression were observed (Sato, Fujikado, Lee et al., 2008; Sato, Fujikado, Morimoto et al., 2008). Calcium plays an extensive and critical role in retinal physiology, including modulating signaling pathways in cell death and the release of protective neurotrophic factors. To make use of the above mentioned findings, a 5 Hz sinusoidal stimulation waveform was chosen for the present study.

Similar to the work presented here, several investigations focus on the retina itself. Politis, Zanakis, and Albala (1988) showed that chronic DC currents promoted a regenerative response in mammalian optic nerve. Morimoto, Fujikado, and Fukuda (2002) and Morimoto et al. (2010) presented extensive work on the survival rates of axotomized retinal ganglion cells after chronic pulsed biphasic electrical stimulation. Morimoto's group found that transcorneal electrical stimulation (TES) rescued the axotomized retinal ganglion cells, likely by activating endogenous retinal IGF-1 system (Morimoto et al., 2005; Tagami et al., 2009). In a related study, TES was associated with a preservation of outer nuclear layer thickness in RCS rats up to 9 weeks of age (end of study period), but the functional benefit observed in this study was transient (Morimoto et al., 2007). Preservation of the inner nuclear layer in isolated RCS rat retina was associated with delivery of monophasic transretinal stimulation (20 Hz, 2.5–10.7 nC per phase) (Schmid et al., 2009). The TES system was also investigated in patients with ischemic optic neuropathy and traumatic optic neuropathy, and was reported to benefit visual acuity and visual field responses (Fujikado et al., 2006).

Chow et al. (2004) demonstrated clinical evidence that chronic electrical stimulation of the retina in patients blinded by retinitis pigmentosa (RP) results in improved vision. This particular study involved six patients with RP who received a silicon-based chip containing micro-photodiodes placed in the subretinal space. The currents were generated in response to natural illumination of the back of the eye, and were below threshold for directly activating second-order neurons of the diseased retina. The frequency spectrum of the currents were determined by the temporal variations in natural retinal illuminance, which is determined by temporal changes in the visual scene; this can be estimated to be significantly less than 30 Hz, the frequency at which flicker-fusion occurs, and probably close to 1 Hz, a typical frequency for saccadic eye movements. More recently, TES was explored for safety and efficacy in a small population of RP patients that were treated 30 min per week for six weeks (biphasic 20 Hz pulses, amplitudes above and below phosphene threshold), with positive results in visual field and *b*-wave amplitude.

The early results in human patients described above motivated an animal study using subretinal implants based on the same photodiode technology (Pardue et al., 2005). Here, RCS rats received an active implant in one eye, with the opposite eye serving as one of three control types (inactive implant, sham surgery, no surgery). Animals receiving active implants demonstrated a temporary (4–6 weeks post surgery) improvement in function, measured by the ERG b-wave amplitude, which disappeared by 8 weeks post surgery, relative to all three control groups. Animals receiving either an active or passive device demonstrated a relative preservation of photoreceptor cells in the vicinity of the implant, relative to the sham surgery and no surgery control eyes. The currents generated by the photoelectric Chow-type implant were reported to be approximately 0.01–1 $\mu A\,cm^{-2}$ modulated (by the investigators) at 120 Hz under ambient fluorescent light levels, but these numbers are estimates made without consideration of actual retinal illuminance or *in vivo* load impedance seen by the implant. More recently, Ciavatta et al. (2009) found increased FGF2 expression and larger ERG b-waves in RCS rats with subretinal implants, relative to control animals similar to those described above. An extensive micro-array gene expression profiling study was reported for wild-type rats following a single TES session (1 h, 20 Hz biphasic pulses, 200 μA), demonstrating differential expression of several potentially neuroactive genes, in particular the down regulation of proapoptotic *Bax* (Willmann et al., 2011).

2. Methods

2.1. Animals

The P23H transgenic rat mimics autosomal dominant retinitis pigmentosa (adRP) retinal degeneration characteristics (Machida et al., 2000; Hafezi et al., 2000; Marc & Jones, 2003). P23H is a point mutation in the opsin gene in which cysteine is replaced by adenine, leading to the substitution of histodine for proline, at the 23rd position, on the rhodopsin protein. The specific line of animals used in this study, line 1 homozygous P23H rat (on an albino background, provided by Dr. Mathew LaVail, UCSF), were bred with pigmented WT Long Evans rats to produce a pigmented P23H heterozygous model that has a single P23H transgenic allele in addition to the normal two wild-type opsin alleles. In albino heterozygotes, the outer nuclear layer (ONL) degenerates rapidly between 4 and 8 weeks of age, has degenerated to less than 30% of normal counts by 16 weeks, and by 29 weeks the ONL has fewer than two rows of cells remaining, representing less than 10% of normal ONL thickness (Machida et al., 2000). Degeneration rates are somewhat slower for the pigmented animals used in this work, with photoreceptor loss of 40–60% by 16 weeks of age (Sekirnjak et al., 2009).

2.2. Exogenous currents

Transcorneal electrical stimulation (TES) was delivered to the left eye between sintered Ag/AgCl pellet electrodes, one placed centrally on the cornea, and a second oral electrode was placed between the left cheek and gum. Care was taken to ensure that the corneal electrode did not directly contact the cornea surface, but instead made electrical contact through a film of artificial tears (Baush and Lomb).

The exogenous current source was fabricated by adding a voltage-to-current conversion circuit (precision op amp BB OPA27GP) to a standard function generator (BK Precision, model 4011A), which then supplied a controlled 5 Hz sinusoidal current to the range of expected loads, up to the limit of the operational amplifier (4.7 mA). The load is the impedance between the electrodes contacting the rat. This impedance was measured in three rats under conditions of varying degree of wetness of the eye (artificial tears), which influenced the impedance of the electrode-cornea interface, and over a range of frequencies. The impedance was found to vary

from approximately 20–200 kΩ, typically 40–50 kΩ at the frequency relevant to the present study, 5 Hz.

Delivery of TES currents was performed twice per week for 30 min per session, beginning at 4 weeks of age, and continuing until the endpoint of the study at 16 weeks of age. Animals were anesthetized via intraperitoneal injection of Ketamine and Acepromazin (100 and 2 mg (kg body wt)$^{-1}$, respectively). The cornea was anesthetized with a drop of 1% proparacaine (Baush and Lomb). Commercial heating pads (Sunbeam Health) kept the rats warm during TES. There were six animals in the treated group, and 10 in the control group. Control animals underwent the same anesthetic routine and electrode placement as treated animals, but the electrodes were not connected to a current source. All procedures were in accordance with the ARVO Statement for the Use of Animals in Ophthalmic and Visual Research.

2.3. Selection of current levels

TES current levels were chosen to be below threshold for directly modulating membrane potentials and transmitter release at levels typical of visual scene processing. This was assessed indirectly by measuring the degree of desensitization to photic stimuli immediately following delivery of TES currents. In pilot studies, it was found that exogenous current delivery could reduce a-wave and b-wave amplitudes by as much as 70%, in a manner dependent on duration of current delivery (data not included here). After cessation of current delivery, responses to flash stimuli recovered on a time scale similar to that of dark adaptation. Current levels of approximately 1.0, 5.5 and 16 μA peak to peak (p–p) were considered for the present experiments, chosen to be well below levels found in pilot work to desensitize the retina. Following a 1-h period of dark adaptation, flashes of 0.01, 54, and 2005 sc cd s m^{-2} were delivered at 2-min intervals to obtain baseline values for a-wave and b-wave amplitudes. Maintaining dark conditions, exogenous currents were then delivered for 30 min, followed immediately by repeating the ERG measurements.

None of the three current levels investigated here resulted in significant reductions in a-wave or b-wave amplitudes (data not shown; $p > 0.3$ and $p > 0.6$, respectively); slight decreases in a-wave and b-wave peak times were noted at the 16 μA current level (10% and 17% decrease, respectively), similar to those seen in response to very mild light-adaptation of the retina. A current of 1.5 μA p–p was chosen for this study.

The current delivered was 1.5 μA p–p (1.06 μA root mean squared, RMS) at the electrode interface. Estimated charge density at the retinal surface is 0.06 μC cm^{-2} per phase. This estimate was made by assuming all current traversed the retina, and integrating the area under the current vs. time curve of the waveform for ½ period, and dividing this charge by the estimated area of the retina (0.769 cm^{-2}).

2.4. Electroretinogram measurement

The measured ERG response was used to assess retinal function during the 12 week study, in both treated (TES) and control groups. All TES currents and ERG measurements involved the left eye; TES treatment and ERG measurement were never performed on the same day. Animals were dark adapted longer than 2 h before ERG measurements. Under dim red light, the rat was anesthetized by an intraperitoneal (IP) injection of Ketamine and Xylazine (100 and 5 mg (kg body wt)$^{-1}$, respectively). A boost of anesthetic (1/4–1/3 of the initial dose) was delivered subcutaneously approximately 45 min after the initial dose or as needed; the duration of a typical experiment was 60–90 min. Body temperature was maintained at 37 °C by a regulated heating pad (TR-100, Fine Science Tools). The animal was positioned with the left eye facing the light source (backlit screen). The cornea was anesthetized with 0.5% proparacaine HCl (Baush and Lomb), and pupil dilated using 2.5% Phenylephrine HCl (Baush and Lomb) and 1% Tropicamide (Baush and Lomb). The corneal surface was kept moist with artificial tears (Baush and Lomb) throughout the experiment.

Flash stimuli (0.01, 2.6, 12, 54, 886, 2005 sc cd s m^{-2}) were delivered in a semi-random order at 2-min intervals (each flash strength delivered three times). Flash strengths reflect averaged values from calibration measurements taken near the beginning and end of the study using a photometer (International Light Model IL-1800, SED#100 photodiode detector, R#485 radiance barrel, ZCIE#19555 scotopic filter), which allowed direct calibration in scotopic candela seconds per square meter (sc cd s m^{-2}). All flashes were generated by a photographic flash unit (1000VR power pack, 2140-C flash head, Novatron of Dallas), flash duration of approximately 1 ms. Strength of the stimulus was regulated by aperture filters placed between the lamp and the backlit screen. The interval between flashes, 2 min, was long enough for the eye to recover from the brightest flash.

ERG responses were recorded using a stainless steel wire loop electrode placed gently on the corneal surface. Two platinum subdermal needle electrodes (E2-48″, Astro-Med Grass) served as reference, placed in the cheek and ground, placed under the skin by the nape of the neck. All electrodes were connected to a differential AC amplifier (P511, Astro-Med Grass), where the signal was amplified 1000× with 0.1–300 Hz pass band (−6 dB). The output signal from the amplifier led to an A/D board in a PC where the data were sampled at a rate of 1 kHz. Custom software (written in DTV, Hewlett Packard) was used for data collection and control of stimulus timing.

2.5. ERG data analysis

ERG a-wave and b-wave amplitudes were normalized to the amplitude of the response elicited with the strongest stimulus, which was above saturation, and used to generate amplitude–intensity plots. The Naka-Rushton equation (Eq. (1)) was fit to the data, and the stimulus strength required to elicit a half-saturated response, $I_{1/2}$, was taken as a measure of rod sensitivity (Evans, Peachey, & Marchese, 1993). All analysis was performed using SigmaPlot 2000 software.

$$A/A_{\max} = I^n/(I^n + I_{1/2}^n) \quad (1)$$

where A is the a-wave amplitude in response to stimulus of strength I; $A_{\max}$ is the maximum a-wave amplitude (response to 2005 sc cd s m^{-2}); n is the nonlinearity constant, set to 1 for the present analysis; I is the flash strength (sc cd s m^{-2}); $I_{1/2}$ is the free parameter in the least-squares fit.

The normalized ERG waveforms were analyzed by fitting Eq. (2) to the leading edge of the a-waves obtained in each experiment.

$$\frac{A}{A_m} = \exp\left[\gamma I_{test}\alpha(t - t_d)^2\right] \quad (2)$$

Eq. (2) is similar to the expression derived by Lamb and Pugh (1992, 2006) to describe the time course of the change in rod circulating current following a flash stimulus. Here, the flash strength (I_{test}, in sc cd s m^{-2}) is multiplied by an arbitrary scaling factor, γ (=1000 in all fits). In the present fits, the delay time t_d was fixed at 3.1 ms, and the amplification constant α was the free parameter. Waveforms obtained in a single experiment were averaged for repeated presentations of the same stimulus strength, and the fit of Eq. (2) performed to the ensemble of four average waveforms (one waveform for each of the four highest flash strengths), resulting in a single value of α for each experiment. The ensemble of waveforms for each experiment was normalized to the a-wave peak

for the response to the highest flash strength; the time of peak was determined from the averaged response taken across all experiments under a given condition. The fit was performed for the segment of each waveform extending from $t = 3$ ms (the approximate post-stimulus time at which responses depart from baseline) to a time just preceding the a-wave peak for that response, which was evaluated for each individual waveform. The quality of the fit was evaluated using the correlation coefficient r^2, and the values of α were then averaged across experiments for comparison between experimental groups (TES treated and control) and ages (4–16 weeks). It has been noted that the value of the amplification constant decreases for responses to very bright flashes; no attempt was made to fit Eq. (2) for individual flash strengths.

2.6. Histology

After the 16 week ERG measurements (20 weeks of age), animals were sacrificed using CO_2 asphyxiation. The eyes were immediately injected with 0.1 mL of a standard 1% paraformaldehyde (FA)/2.5% glutaraldehyde (GA) fixative solution using a 26G needle inserted nasally through the limbus. The enucleated eyes were immersed in ~2.0 mL of fixative solution, stored in 2 mL centrifuge tubes. The samples were then sent to the Moran Eye Center in Salt Lake City, Utah, for histological analysis (Marc, Murry, & Basinger, 1995; Marc et al., 2003; Jones et al., 2003). Briefly, all samples were processed in resin matrices for thin sectioning. Two key parameters were measured for this study: the thickness of the outer nuclear layer (ONL), and the distance between the external limiting membrane (ELM) and retinal pigment epithelium (RPE), as an estimate of the outer segment layer thickness (OSL). Each image was captured using Nomarski optics (Zeiss 40x planapochromatic) by a Dage-MTI camera at 221 nm/pixel resolution.

2.7. Statistical analysis

Statistical analysis was performed with commercial software (Excel for Windows). In general, associations between two numerical variables of independence were examined by using Student's paired t-test. The criterion of significance was assessed at the $p < 0.02$ level.

3. Results

3.1. Photoreceptor responses

ERG a-waves were analyzed for maximum amplitude elicited by the saturating 2005 sc cd s m^{-2} stimulus as an index of massed photoreceptor activity. The top panel in Fig. 1 plots the mean a-wave amplitudes as a function of age for the treated and control animals. There was no significant difference at any age ($p > 0.09$), though at 4 weeks, the mean amplitude for the control group was larger than the treated group. The treated and control animals were typically littermates, and the 4 week responses were recorded before the first TES session; the difference at 4 weeks appears to be due to chance. To correct for the pre-TES difference between groups, the lower panel of Fig. 1 plots the same amplitudes after normalizing to the value obtained at 4 weeks in each group. At 16 weeks of age, the ERG a-wave for the treated animals was reduced to ~32% of the 4 week amplitude, and to ~24% for the control group. The normalized data reveal a statistically significant difference between stimulated and control group at 16 weeks of age, with the treated animals exhibiting higher amplitudes ($p < 0.02$, 95% power).

The a-wave amplitudes within each experiment were normalized to the response to the brightest flash and plotted vs. flash strength at each age investigated (4, 8, 12 and 16 weeks). These amplitude–intensity plots were then averaged across all animals in each group at 4 weeks and 16 weeks; these are shown in the upper and lower panels of Fig. 2, respectively. The responses obtained from each animal were fit with Eq. (1); goodness of fit was evaluated by calculating the correlation coefficient r^2, which ranged from 0.83 to 0.94. The mean $I_{1/2}$ values at each age were used to plot Eq. (1) as the curves in Fig. 2. At 16 weeks, the curve describing the control animals shifted significantly to the right, indicating reduced sensitivity, while the curve describing the TES treated animals was unchanged from the 4 week curve.

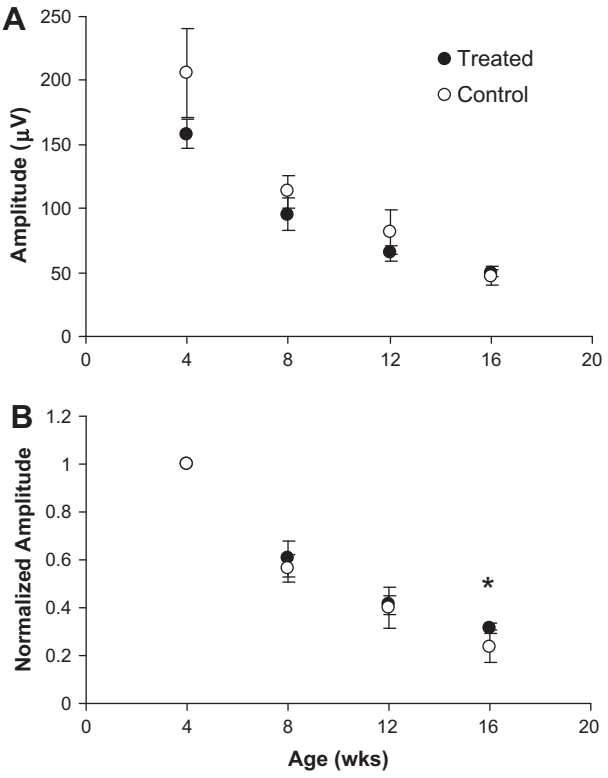

Fig. 1. Maximum ERG a-wave amplitudes vs. age. Responses elicited with the highest flash strength (2005 sc cd s m^{-2}) and evaluated at peak. Values for TES treated animals ($n = 6$) plotted with filled circles (●); control data ($n = 10$) plotted with open circles (○); error bars indicate +1 standard deviation. (A) Mean absolute amplitudes. (B) Mean amplitudes normalized to the value recorded at 4 weeks of age. Asterisk indicates significant difference (t-test, $p < 0.02$, 95% power).

The mean $I_{1/2}$ values are plotted vs. age in Fig. 3. The half-saturating flash strength increased with age for the control group, and remained nearly constant for the treated group, resulting in significant differences at 8, 12 and 16 weeks of age.

Week 4:
0.97 + 0.02 (range 0.92–0.99)
Week 16:
0.91 + 0.03 (range 0.84–0.97)

To further explore the apparent difference in photoreceptor sensitivity, the leading edge of the a-waves obtained in each experiment (i.e., each individual animal at each age) were analyzed with Eq. (2). Representative ensemble fits are shown in Fig. 4. Fits to the responses were generally good, with the mean (±1 SD) r^2 value of 0.97 + 0.02 (range 0.92–0.99) for responses recorded at 4 weeks of age, and 0.91 + 0.03 (range 0.84–0.97) at 16 weeks of age. Due to the low sampling rate (1 kHz) and small amplitude of the re-

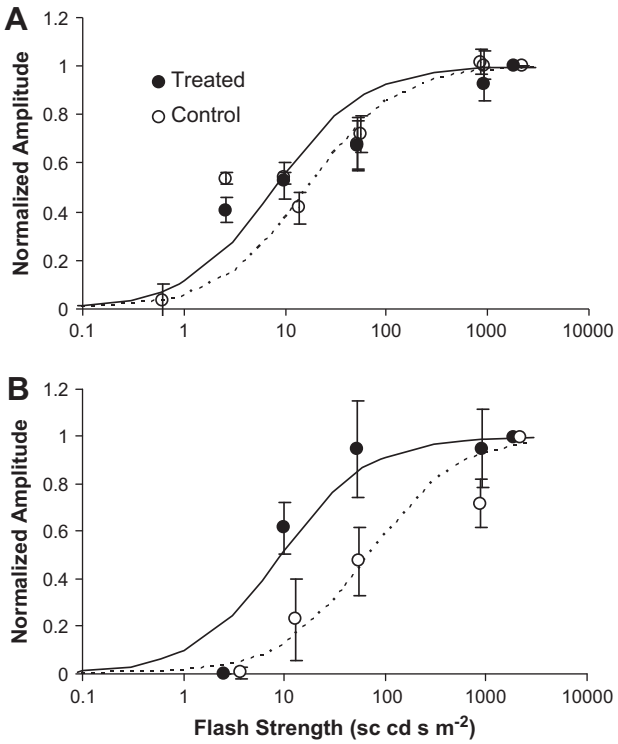

Fig. 2. Normalized ERG a-wave amplitudes vs. flash strength. Responses normalized to the response to the highest flash strength obtained in each experiment, and evaluated at peak. Values for TES treated animals ($n = 6$)plotted with filled circles (●); control data ($n = 10$) plotted with open circles (○); error bars indicate +1 standard deviation. Curves plot Eq. (1), using the mean value of $I_{1/2}$ obtained across all animals in each group. Solid and dashed curves fit to data from treated and control groups, respectively. (A) Amplitude–intensity plots obtained at 4 weeks of age, before the first TES session. Values of r^2 describing fit of Eq. (2) to treated and control data are 0.90 and 0.94, respectively. (B) Amplitude–intensity plots obtained at 16 weeks of age, after 12 weeks of TES treatment. Values of r^2 describing fit of Eq. (2) to treated and control data are 0.94 and 0.83, respectively.

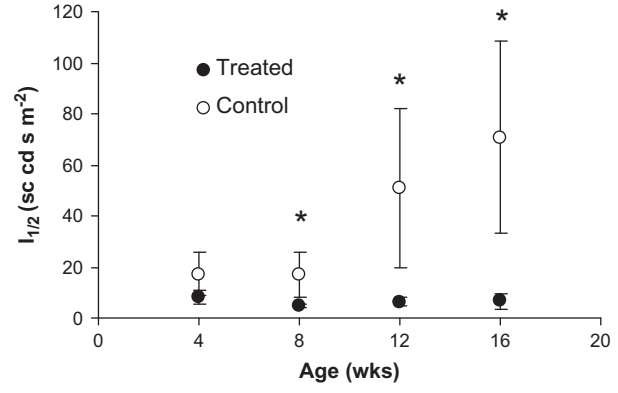

Fig. 3. Flash strength required to reach half-saturation of the a-wave ($I_{1/2}$) vs. age. Values for TES treated animals ($n = 6$) plotted with filled circles (●); control data ($n = 10$) plotted with open circles (○); error bars indicate +1 standard deviation. Asterisk indicates significant difference (t-test, $p < 0.02$).

sponses at 16 weeks (~50 μV max) the normalized responses used for the fits appear quite noisy at this age (right panels of Fig. 4). The mean values of the sensitivity constant α for each group at 4 and 16 weeks of age are summarized in Table 1. The control group showed no significant change in α over the ages investigated, while the treated group exhibited a decrease that was on the margin of significance.

3.2. Bipolar cell responses

The dominant contributor to the ERG b-wave is ON-bipolar cell activity (Cameron, Mahroo, & Lamb, 2006). The peak amplitudes of the ERG b-waves obtained in response to the saturating 2005 sc cd s m^{-2} stimulus were analyzed at each age, and are plotted in Fig. 5. The upper panel of Fig. 5 plots the averaged raw amplitudes; significant differences were found at 12 and 16 weeks of age, where the TES treated animals exhibited larger b-wave responses than control animals ($p < 0.005$). For consistency with the analysis of the a-wave amplitudes, the b-wave amplitudes were also normalized to the values obtained at 4 weeks in each animal, and replotted in the lower panel of Fig. 5.

The relative preservation of b-wave amplitudes in TES treated animals, taken with the similar decrease in a-wave amplitudes for both treated and control groups, suggests a preservation of photoreceptor-bipolar cell coupling. To illustrate this phenomenon, the ratio of mean normalized amplitudes (b-wave)/(a-wave) was calculated at each age; these are plotted in Fig. 6. The ratio for the control group was weakly correlated with age ($r^2 = 0.47$; slope = 0.02 $week^{-1}$, least squares linear regression analysis), while the ratio for the treated group increased steadily with age for the duration of the study ($r^2 = 0.98$; slope = 0.07 $week^{-1}$). At 16 weeks of age, the ratios for the control and treated groups were 1.3 and 1.8, respectively. The ratio for the treated group at 16 weeks of age was nearly twice that found at 4 weeks of age (1.8 vs. 1).

3.3. Histology

At 16 weeks of age, the eyes were coded and sent to the Marc laboratory for a blind analysis of the anatomical differences between the treated and control groups. The upper panel of Fig. 7 shows representative samples of control and TES treated retinal sections. The lower panel of Fig. 7 plots the combined thickness of the outer nuclear layer (ONL) and outer segment layer (OSL) in control and TES animals. There is no statistical difference between the groups ($p > 0.2$, power = 70%, $n = 6$ in each group). The ONL + OSL thickness was also evaluated in the non-treated eye (OD) of the animals in the treated group, which showed no difference from the treated eye (not shown).

4. Discussion

Gross histological examination revealed no significant preservation of cell numbers or rod outer segment length associated with TES treatment; in both treated and control groups these measures decreased with age on the time course expected for the pigmented line 1 P23H rats. However, ERG measurement and analysis revealed functional differences after 8–12 weeks of TES treatment. The observed differences between control and treated animals suggest an overall benefit resulting from the TES currents. The functional benefit increased with age over the period investigated, in contrast to previous studies demonstrating functional improvements that appeared to be transient (Pardue et al., 2005; Morimoto et al., 2007). Distinct features of the present study are TES wave shape (controlled sinusoidal current) and electrode location (placed on the eye and in the mouth).

The most striking difference between treated and control animals was the measure of photoreceptor sensitivity, $I_{1/2}$. This value increased with age in control animals (implying decreasing sensitivity), but was preserved at 4 week values throughout the study in treated animals (Fig. 3). Machida et al. (2000) reported a continuous but statistically insignificant increase in $I_{1/2}$ in albino line 1 P23H rats between 4 and 29 weeks of age, though a post hoc power analysis revealed insufficient sample sizes. A second point of differ-

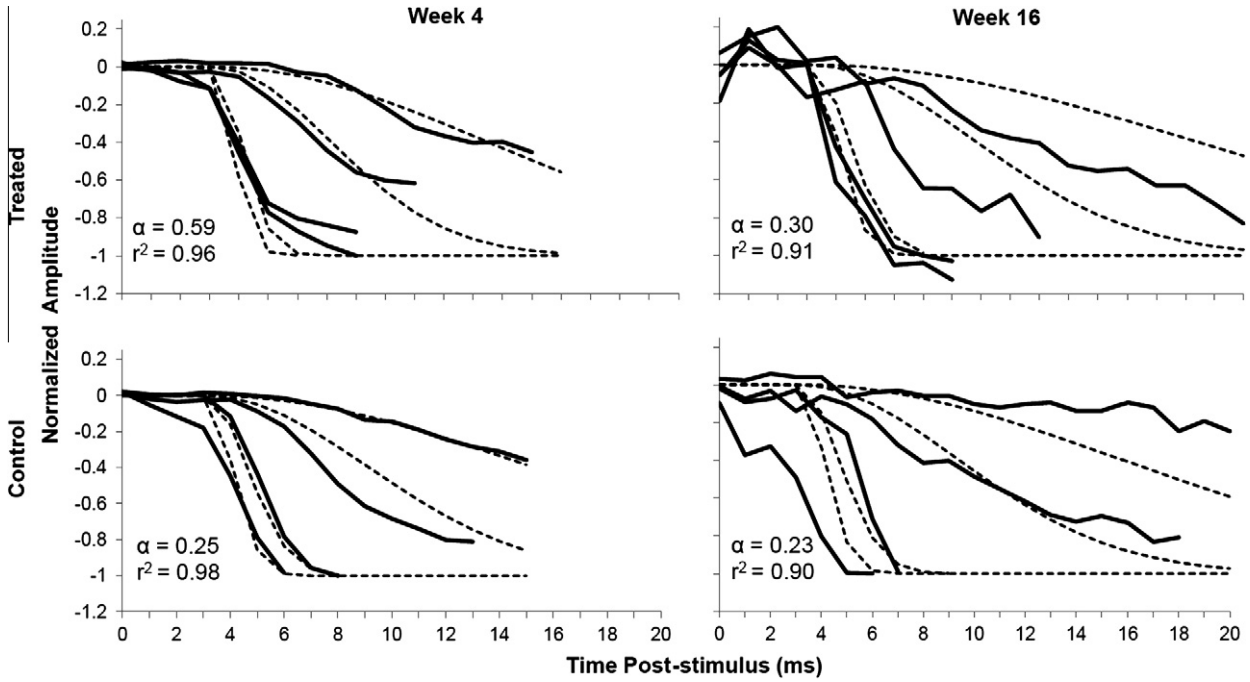

Fig. 4. Representative fits of Eq. (2) for two animals (one treated, one control). Normalized ERG response waveforms (solid lines) and Eq. (2) fitted to the ensemble of responses in each plot (dashed lines); values of free parameter α and measure of quality of fit (r^2) given in each panel. Stimulus strengths were 12, 54, 886 and 2005 sc cd s m^{-2}. Responses recorded at 4 weeks of age (left) and 16 weeks of age (right).

Table 1
Summary of the parameter α, an index of the gain of phototransduction. Student's *t*-test used to calculate *p*-values; post hoc power analysis.

	Control 4 week vs. 16 week	Treated 4 week vs. 16 week
α (Mean + 1 SD)	0.31 + 0.14 vs. 0.27 + 0.11	0.51 + 0.22 vs. 0.32 + 0.03
p-Value (power)	0.51 (10%)	0.06 (62%)

ence between treated and control data sets in the present study was a much higher inter-animal variation in $I_{1/2}$ observed in the control group compared to treated animals (one standard deviation = 38 vs. 3 sc cd s m^{-2}, respectively). The higher variability in control animals was not due to an underlying higher variability in a-wave response amplitudes (i.e. "noisier" data), and appears to reflect inter-animal differences in sensitivity.

The value of $I_{1/2}$ reflects the number of incident photons required to reach a half-saturated a-wave amplitude, and is determined primarily by two contributing quantities: (1) the efficiency with which rhodopsin is photoisomerized (R^*/photon); and (2) the gain relating number of photoisomerizations to changes in circulating current (described by the amplification constant, α). Changes in $I_{1/2}$ therefore imply changes in one or both of these related quantities. Because $I_{1/2}$ and α were determined through analysis of the recorded a-waves, it is possible to speculate on changes in R^*/photon. This line of thought is summarized in Table 2.

Consistent with the present results, previous reports found that the value of the amplification constant does not change over time in RP patients (annual retest over 4 year period (Birch, Hood, & Locke, 2002)) or as a function of disease stage in Abyssinian cats (a model of RP-like degeneration (Kang Derwent et al., 2006)). The decrease in sensitivity (increase in $I_{1/2}$) observed here in control animals, taken with the constancy of α in this group, suggests that the shift in the amplitude–intensity curve (Fig. 2) is due to a decrease in photoisomerization efficiency.

The near-constant value of $I_{1/2}$ observed in treated animals, taken with the observed decrease in α in this group, suggests that an increase in photoisomerization efficiency was associated with the delivered currents. In a previous study, the amplification

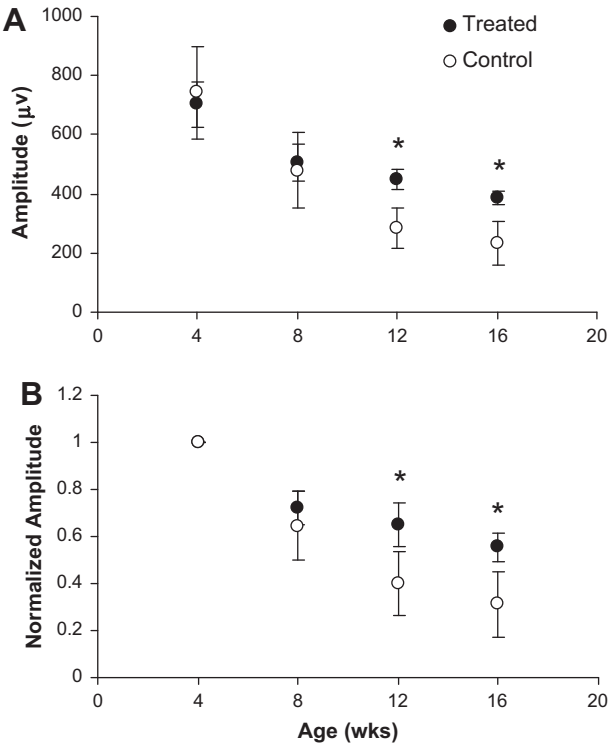

Fig. 5. Maximum ERG b-wave amplitudes vs. age. Responses elicited with the highest flash strength (2005 sc cd s m^{-2}) and evaluated from trough of a-wave to peak of b-wave. Values for TES treated animals plotted with filled circles (●); control data plotted with open circles (○); error bars indicate +1 standard deviation. (A) Mean absolute amplitudes. (B) Mean amplitudes normalized to the value recorded at 4 weeks of age. Asterisk indicates significant difference (*t*-test, $p < 0.005$). Six treated eyes and ten control eyes analyzed.

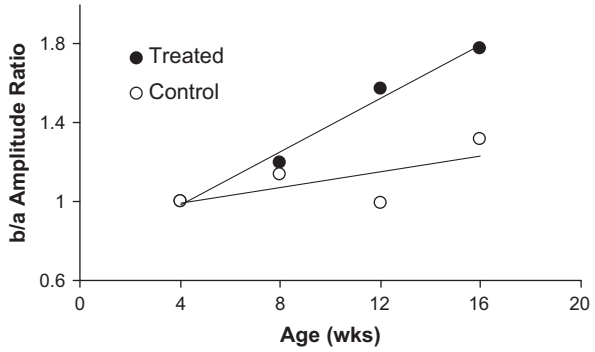

Fig. 6. Ratio of ERG b-wave and a-wave amplitudes (b/a) vs. age. Values for TES treated animals plotted with filled circles (●); control data plotted with open circles (○). Lines plot results from a least-squares linear regression analysis. Slope and r^2 values for data from treated group: 0.07 week^{-1}, 0.98. For control group: 0.02 week^{-1}, 0.47. Six treated eyes and 10 control eyes analyzed.

constant in P23H rats was found to be higher than in wild-type control animals (Machida et al., 2000), possibly a compensatory response to reduced photon capture. The amplification constant in RP patients was found to be within, or well below, the normal range (Shady, Hood, & Birch, 1995). The decrease in α over time observed in treated animals in the present study may be a direct negative effect of the TES currents, or a shift toward wild-type values subsequent to the suggested increase in R^*/photon. This idea requires that the retina is able to sense photoisomerization efficiency, i.e., sense incident photons by means other than photoisomerization of rhodopsin, perhaps by intrinsically photosensitive ganglion cells (Hattar et al., 2002; Berson, Dunn, & Takao, 2002). The rats in this study carried one copy of the mutant transgene and two copies of the wild-type gene. Photoisomerization efficiency could be modulated through enhanced expression of the wild-type rhodopsin gene, or suppression of the mutated rhodopsin gene; regulation of gene expression via exogenous currents has been documented in retina and retinal cells (Sato, Fujikado, Lee et al., 2008; Sato, Fujikado, Morimoto et al., 2008; Ciavatta et al., 2009; Willmann et al., 2011), as well as other contexts (Al-Majed, Tam, & Gordon, 2004). Many neuroprotective mechanisms, both cellular and molecular, have been associated with electrical activity in neurons induced by exogenously applied fields or currents (reviewed by Corredor and Goldberg (2009)); effects on photoreceptors are most likely explained by effects on membrane potential and calcium conductance (as opposed to synaptic feedback mechanisms). Calcium can modulate gene expression, and plays an intimate role in regulating phototransduction (Stephen et al., 2008).

Table 2
Direction of relative change in three quantities describing photoreceptor function between 4 and 16 weeks of age. In the control and TES columns, entries in rows two and three should explain the entry in row one. Entries in rows one and two were based on experimental measurement; entries in row three are implied from interpretation of rows one and two.

	Control	TES treated
Sensitivity (observed $I_{1/2}$)	Decreased	No change
Amplification (observed α)	No change	Decreased
R^*/photon (*implied*)	Decreased	Increased

The uncoupling of bipolar cell dendrites from photoreceptors (Marc & Jones, 2003; Marc et al., 2003) results in a decrease of b-wave amplitudes, which lags the decrease in a-wave amplitudes.

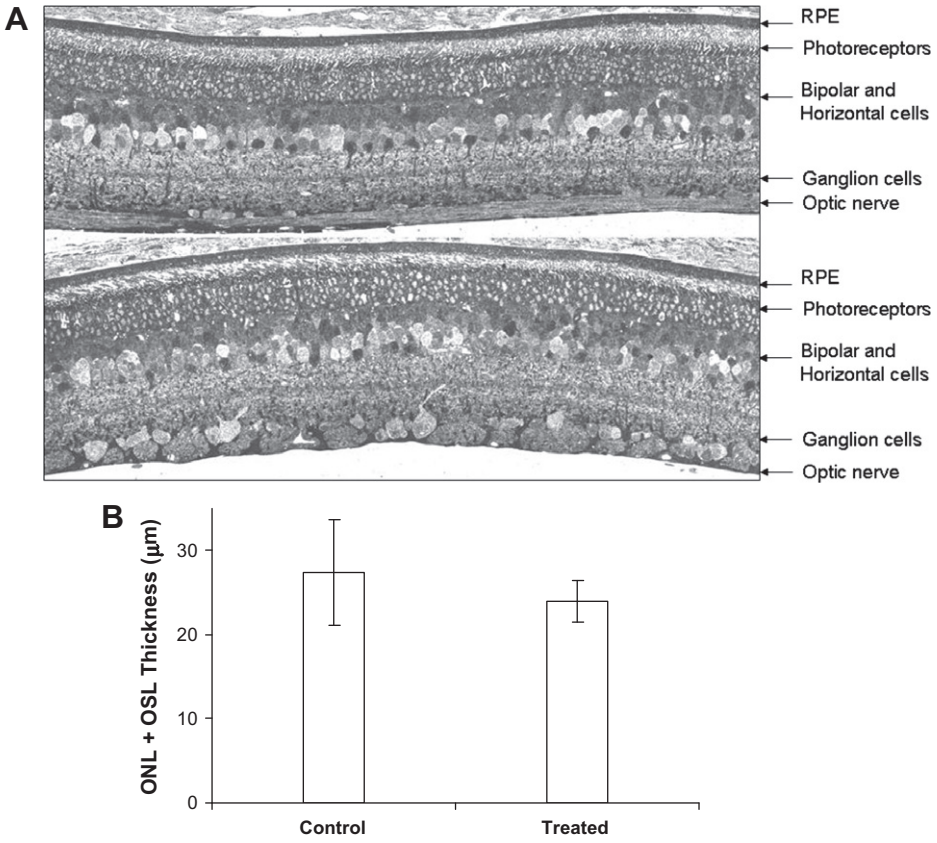

Fig. 7. Results from histological evaluation at 16 weeks of age in TES treated and control groups. (A) Representative thin sections from one control animal (top) and one TES treated animal (bottom). Primary retinal structures as labeled. (B) Mean combined thicknesses of the outer nuclear layer (ONL) and outer segment layer (OSL); error bars indicate +1 standard deviation. There was no significant difference between groups.

The decrease in a-wave amplitudes was similar in both groups. The b-wave amplitudes in both treated and control groups also decreased over the 12-week study period, but with different time courses. The ratio of b-wave to a-wave amplitudes increased steadily in treated animals from 4 to 16 weeks of age, suggesting a delay in the rate of bipolar cell retraction from photoreceptors (Fig. 6). In early-stage degeneration, horizontal cells also retract from photoreceptors, removing inhibitory feedback (Jones & Marc, 2005), and it is conceivable that TES treatment accelerated this process; however complete ablation of horizontal cells in adult mice was associated with proportionally larger losses in b-wave amplitudes than a-wave amplitudes (Sonntag et al., 2012). It is important to note that b-wave amplitude preservation was associated with preserved photoreceptor sensitivity ($I_{1/2}$), but not absolute amplitudes of the photoreceptor response, and in the presence of a reduced phototransduction amplification constant. These results suggests that network function in the retina was relatively preserved in the TES treated group, and that bipolar cell retraction from photoreceptors may be sensitive to the overall gain of photoreceptors (change in transmitter release per incident photon) but not the gain of phototransduction (change in circulating current per photoisomerization).

5. Summary

The potentially therapeutic effects of chronic exogenous currents delivered to the eye were investigated in the pigmented P23H rat. No significant difference in photoreceptor numbers, outer segment lengths, or ERG a-wave amplitudes were found between TES treated and control groups. The stimulus strength required to elicit a half-saturating a-wave ($I_{1/2}$) increased with age in control animals, but was nearly constant in treated animals. This measure of sensitivity, taken with the observed decrease in the phototransduction amplification constant in treated animals, suggests that preservation of sensitivity was mediated by an increase in efficiency of photoisomerization. The ratio of b-wave to a-wave amplitudes increased with age, suggesting that retraction of bipolar cells from degenerating photoreceptors is delayed when photoreceptor sensitivity is preserved.

Acknowledgments

The authors would like to thank Drs. Robert Marc and Bryan Jones of the Moran Eye Institute at the University of Utah for their histological analysis and intellectual support. This work was funded by a research contract with OcuMed, Inc., and by a research fellowship and Novak Family Grant from Fight for Sight. L. Bogdanowicz has a financial interest in OcuMed, Inc.

References

Al-Majed, A. A., Tam, S. L., & Gordon, T. (2004). Electrical stimulation accelerates and enhances expression of regeneration-associated genes in regenerating rat femoral motoneurons. *Cellular & Molecular Neurobiology, 24*(3), 379–402.

Berson, D. M., Dunn, F. A., & Takao, M. (2002). Phototransduction by retinal ganglion cells that set the circadian clock. *Science, 295*(5557), 1070–1073.

Birch, D. G., Hood, D. C., & Locke, K. G. (2002). Quantitative electroretinogram measures of phototransduction in cone and rod photoreceptors. Normal aging, progression with disease, and test-retest variability. *Archives of Ophthalmology, 120*, 1045–1051.

Borgens, R. B. (1999). Electrically mediated regeneration and guidance of adult mammalian spinal axons into polymeric channels. *Neuroscience, 91*(1), 251–264.

Borgens, R. B., Blight, A. R., & McGinnis, M. E. (1987). Behavioral recovery induced by applied electric fields after spinal cord hemisection in guinea pig. *Science, 238*(4825), 366–369.

Borgens, R. B., & Bohnert, D. M. (1997). The responses of mammalian spinal axons to an applied DC voltage gradient. *Experimental Neurology, 145*(2 Pt 1), 376–389.

Brushart, T. M., Hoffman, P. N., Royall, R. M., Murinson, B. B., Witzel, C., & Gordon, T. (2002). Electrical stimulation promotes motoneuron regeneration without increasing its speed or conditioning the neuron. *The Journal of Neuroscience, 22*(15), 6631–6638.

Cameron, A. M., Mahroo, O. A., & Lamb, T. D. (2006). Dark adaptation of human rod bipolar cells measured from the b-wave of the scotopic electroretinogram. *Journal of Physiology, 575*(Pt 2), 507–526.

Cheng, W. L., & Lin, C. C. (2004). The effects of different electrical stimulation protocols on nerve regeneration through silicone conduits. *Journal of Trauma-Injury Infection & Critical Care, 56*(6), 1241–1246.

Cho, M. R., Marler, J. P., Thatte, H. S., & Golan, D. E. (2002). Control of calcium entry in human fibroblasts by frequency-dependent electrical stimulation. *Frontiers in Bioscience, 7*, a1–a8.

Cho, M. R., Thatte, H. S., Lee, R. C., & Golan, D. E. (2000). Integrin-dependent human macrophage migration induced by oscillatory electrical stimulation. *Annals of Biomedical Engineering, 28*(3), 234–243.

Chow, A. Y., Chow, V. Y., Packo, K. H., Pollack, J. S., Peyman, G. A., & Schuchard, R. (2004). The artificial silicon retina microchip for the treatment of vision loss from retinitis pigmentosa. *Archives of Ophthalmology, 122*, 460–469.

Ciavatta, V. T., Kim, M., Wong, P., Nickerson, J. M., Shuler, R. K., Jr., McLean, G. Y., et al. (2009). Retinal expression of Fgf2 in RCS rats with subretinal microphotodiode array. *Investigative Ophthalmology & Visual Science, 50*(10), 4523–4530.

Cork, R. J., McGinnis, M. E., Tsai, J., & Robinson, K. R. (1994). The growth of PC12 neurites is biased towards the anode of an applied electrical field. *Journal of Neurobiology, 25*(12), 1509–1516.

Corredor, R. G., & Goldberg, J. L. (2009). Electrical activity enhances neuronal survival and regeneration. *Journal of Neural Engineering, 6*(5), 055001 (Review).

Evans, L. S., Peachey, N. S., & Marchese, A. L. (1993). Comparison of three methods of estimating the parameters of the Naka-Rushton equation. *Documenta Ophthalmologica, 84*(1), 19–30.

Fujikado, T., Morimoto, T., Matsushita, K., Shimojo, H., Okawa, Y., & Tano, Y. (2006). Effect of transcorneal electrical stimulation in patients with nonarteritic ischemic optic neuropathy or traumatic optic neuropathy. *Japanese Journal of Ophthalmology, 50*(3), 266–273.

Hafezi, F., Grimm, C., Simmen, B. C., Wenzel, A., & Remé, C. E. (2000). Molecular ophthalmology: an update on animal models for retinal degenerations and dystrophies. *British Journal of Ophthalmology, 84*(8), 922–927.

Hattar, S., Liao, H. W., Takao, M., Berson, D. M., & Yau, K. W. (2002). Melanopsin-containing retinal ganglion cells: Architecture, projections, and intrinsic photosensitivity. *Science, 295*(5557), 1065–1070.

Jones, B. W., & Marc, R. E. (2005). Retinal remodeling during retinal degeneration. *Experimental Eye Research, 81*, 123–137.

Jones, B. W., Watt, C. B., Frederick, J. M., Baehr, W., Chen, C. K., Levine, E. M., et al. (2003). Retinal remodeling triggered by photoreceptor degenerations. *Journal of Comparative Neurology, 464*(1), 1–16.

Kang Derwent, J. J., Padnick-Silver, L., McRipley, M., Giuliano, E., Linsenmeier, R. A., & Narfstrom, K. (2006). The electroretinogram components in Abyssinian cats with hereditary retinal degeneration. *Investigative Ophthalmology and Visual Science, 47*(8), 3673–3682.

Khatib, L., Golan, D. E., & Cho, M. (2004). Physiologic electrical stimulation provokes intracellular calcium increase mediated by phospholipase C activation in human osteoblasts. *FASEB Journal, 18*(15), 1903–1905.

Kubota, K., Yoshimura, N., Yokota, M., Fitzsimmons, R. J., & Wikesjo, M. E. (1995). Overview of effects of electrical stimulation on osteogenesis and alveolar bone. *Journal of Periodontology, 66*(1), 2–6.

Lamb, T. D., & Pugh, E. N. Jr, (1992). A quantitative account of the activation steps involved in phototransduction in amphibian photoreceptors. *Journal of Physiology, 449*, 719–758.

Lamb, T. D., & Pugh, E. N. Jr, (2006). Phototransduction, dark adaptation, and rhodopsin regeneration. The Proctor lecture. *Investigative Ophthalmology and Visual Science, 47*(12), 5138–5152.

Leake, P. A., Hradek, G. T., Rebscher, S. J., & Snyder, R. L. (1991). Chronic intracochlear electrical stimulation induces selective survival of spiral ganglion neurons in neonatally deafened cats. *Hearing Research, 54*, 251–271.

Leake, P. A., Hradek, G. T., & Snyder, R. L. (1999). Chronic electrical stimulation by a cochlear implant promotes survival of spiral ganglion neurons after neonatal deafness. *Journal of Comparative Neurology, 412*, 543–562.

Machida, S., Kondo, M., Jamison, J. A., et al. (2000). P23H rhodopsin transgenic rat: Correlation of retinal function with histopathology. *Investigative Ophthalmology & Visual Science, 41*, 3200–3209.

Marc, R. E., & Jones, B. W. (2003). Retinal remodeling in inherited photoreceptor degenerations. *Molecular Neurobiology, 28*(2), 139–147.

Marc, R. E., Jones, B. W., Watt, C. B., & Strettoi, E. (2003a). Neural remodeling in retinal degeneration. *Progress in Retinal & Eye Research, 22*(5), 607–655 (Review).

Marc, R. E., Murry, R. F., & Basinger, S. F. (1995). Pattern recognition of amino acid signatures in retinal neurons. *Journal of Neuroscience, 15*(7 Pt 2), 5106–5129.

Marqueste, T., Alliez, J. R., Alluin, O., Jammes, Y., & Decherchi, P. (2004). Neuromuscular rehabilitation by treadmill running or electrical stimulation after peripheral nerve injury and repair. *Journal of Applied Physiology, 96*(5), 1988–1995.

Morimoto, T., Fujikado, T., Choi, J. S., Kanda, H., Miyoshi, T., Fukuda, Y., et al. (2007). Transcorneal electrical stimulation promotes the survival of photoreceptors and preserves retinal function in royal college of surgeons rats. *Investigative Ophthalmology & Visual Science, 48*(10), 4725–4732.

Morimoto, T., Miyoshi, T., Fujikado, T., Tano, Y., & Fukuda, Y. (2002). Electrical stimulation enhances the survival of axotomized retinal ganglion cells in vivo. *Neuroreport, 13*(2), 227–230.

Morimoto, T., Miyoshi, T., Matsuda, S., Tano, Y., Fujikado, T., & Fukuda, Y. (2005). Transcorneal electrical stimulation rescues axotomized retinal ganglion cells by activating endogenous retinal IGF-1 system. *Investigative Ophthalmology and Visual Science, 46*, 2147–2155.

Morimoto, T., Miyoshi, T., Sawai, H., & Fujikado, T. (2010). Optimal parameters of transcorneal electrical stimulation (TES) to be neuroprotective of axotomized RGCs in adult rats. *Experimental Eye Research, 90*(2), 285–291.

Ojingwa, J. C., & Isseroff, R. R. (2002). Electrical stimulation of wound healing. *Progress in Dermatology, 36*(4), 1–12.

Pardue, M. T., Phillips, M. J., Yin, H., Sippy, B. D., Webb-Wood, S., Chow, A. Y., et al. (2005). Neuroprotective effect of subretinal implants in the RCS rat. *Investigative Ophthalmology & Visual Science, 46*(2), 674–682.

Politis, M. J., Zanakis, M. F., & Albala, B. J. (1988). Mammalian optic nerve regeneration following the application of electric fields. *Journal of Trauma, 28*, 1548–1552.

Sato, T., Fujikado, T., Lee, T. S., & Tano, Y. (2008). Direct effect of electrical stimulation on induction of brain-derived neurotrophic factor from cultured retinal Muller cells. *Investigative Ophthalmology & Visual Science, 49*(10), 4641–4646.

Sato, T., Fujikado, T., Morimoto, T., Matsushita, K., Harada, T., & Tano, Y. (2008). Effect of electrical stimulation on IGF-1 transcription by L-type calcium channels in cultured retinal Muller cells. *Japanese Journal of Ophthalmology, 52*, 217–223.

Schmid, H., Herrmann, T., Kohler, K., & Stett, A. (2009). Neuroprotective effect of transretinal electrical stimulation on neurons in the inner nuclear layer of the degenerated retina. *Brain Research Bulletin, 79*(1), 15–25.

Sekirnjak, C., Hulse, C., Jepson, L. H., Hottowy, P., Sher, A., Dabrowski, W., et al. (2009). Loss of responses to visual but not electrical stimulation inganglion cells of rats with severe photoreceptor degeneration. *Journal of Neurophysiology, 102*(6), 3260–3269.

Shady, S., Hood, D. C., & Birch, D. G. (1995). Rod phototransduction in retinitis pigmentosa. Distinguishing alternative mechanisms of degeneration. *Investigative Ophthalmology and Visual Science, 36*(6), 1027–1037.

Sonntag, S., Dedek, K., Dorgau, B., Schultz, K., Schmidt, K.-F., Cimiotti, K., et al. (2012). Ablation of retinal horizontal cells from adult mice leads to rod degeneration and remodeling in the outer retina. *The Journal of Neuroscience, 32*(31), 10713–10724.

Stephen, R., Filipek, A., Palczewski, K., & Sousa, M. C. (2008). Ca^{2+}-dependent regulation of phototransduction. *Photochemistry and Photobiology, 2008*(84), 903–910 (Review).

Sun, S., & Cho, M. (2004). Human fibroblast migration in three-dimensional collagen gel in response to noninvasive electrical stimulus. II. Identification of electrocoupling molecular mechanisms. *Tissue Engineering, 10*(9–10), 1558–1565.

Sun, S., Wise, J., & Cho, M. (2004). Human fibroblast migration in three-dimensional collagen gel in response to noninvasive electrical stimulus. I. Characterization of induced three-dimensional cell movement. *Tissue Engineering, 10*(9–10), 1548–1557.

Tagami, Y., Kurimoto, T., Miyoshi, T., Morimoto, T., Sawai, H., & Mimura, O. (2009). Axonal regeneration induced by repetitive electrical stimulation of crushed optic nerve in adult rats. *Japanese Journal of Ophthalmology, 53*(3), 257–266.

Willmann, G., Schäferhoff, K., Fischer, M. D., Arango-Gonzalez, B., Bolz, S., Naycheva, L., et al. (2011). Gene expression profiling of the retina after transcorneal electrical stimulation in wild-type Brown Norway rats. *Investigative Ophthalmology & Visual Science, 52*(10), 7529–7537.